

# Wet scavenging of SO<sub>2</sub> emissions around India's largest lignite based power plant

A. Rai<sup>1</sup>, S. Ghosh<sup>1,3</sup>, and S. Chakraborty<sup>2</sup>

<sup>1</sup>School of Mechanical and Building Sciences, VIT University, India

<sup>2</sup>School of Electrical Sciences, VIT University, India

<sup>3</sup>School of Earth and Environment, University of Leeds, Leeds, UK

Received: 5 September 2009 – Revised: 26 February 2010 – Accepted: 26 February 2010 – Published: 11 March 2010

**Abstract.** The Neyveli Lignite Corporation (NLC) is among the largest lignite based power plants in South East Asia. The four elevated stacks from this power plant emanate a substantial amount of sulphur dioxide into a tropical boundary layer. Sulphur dioxide being a soluble pollutant gas is absorbed by falling raindrops. This is a first study that quantifies the scavenging action of the North Eastern monsoonal rains from a lignite based power plant. We find that although the North Eastern monsoonal rains have a preponderance of very large droplets, the contribution of the small droplets cannot be neglected. We expect that the estimated scavenging coefficients can be used by large eddy and climate models.

## 1 Prevailing meteorology of the Neyveli region

The NLC Township is located on the South Eastern tip of the Indian sub-continent (see Fig. 1). The prevailing winds in Neyveli are mainly South-westerly between May and September and North-westerly during the rest of the year. In this paper our main focus of attention will be on the scavenging action of the North Eastern monsoonal rains. If the monsoon rain water is mixed with oxides of sulphur then it might adversely affect crop production in India. This study will help future quantification of wet removal rates of oxides of sulphur and nitrogen from many other elevated power plant stacks around the country.

Around September, with the sun fast retreating south, the northern land mass of the Indian subcontinent begins to cool off rapidly. With this, air pressure begins to build over northern India. The Indian Ocean and its surrounding atmosphere

still hold its heat. This causes the cold winds to sweep down from the Himalayas and the Indo-Gangetic Plains towards the vast spans of the Indian Ocean south of the Deccan peninsular. This is known as the North-East Monsoon or Retreating Monsoon. While travelling towards the Indian Ocean, the dry cold wind picks up some moisture from the Bay of Bengal and pours it over peninsular India. Cities like Chennai, which get less rain from the South-West Monsoon, receive rain from the Retreating Monsoon. About 50%–60% of the rain received by the state of Tamil Nadu is from the North-East Monsoon – the prevailing wind direction is mainly north easterly (see the Wind Rose in Fig. 2).

Observing Table 1, it is plain that heavy rainfall occurs during the months of October to December, as a result of vigorous NE monsoon activity. Out of the 60 rainy days in a year, the highest rainfall intensity occurs in the month of October over Neyveli. The partitioning of sulphur dioxide between the gas phase and the liquid phase ensures that the dissolved oxides of sulphur are deposited on crops causing them injury and affecting crop production.

## 2 Emissions from NLC

Neyveli is located 160 km from Chennai in the Cuddalore district of Tamil Nadu and NLC is a company promoted by the government of India under the Ministry of Coals. Neyveli Thermal Power Stations are South Asia's first and only lignite-fired Thermal Power Stations and also the first pit-head power stations in India. NLC covers an area of about fifty-four square kilometers, much of which is forested. It mines twenty-four million metric tonnes per annum (MTPA) of lignite, and produces 2,490 megawatts per annum (MW/year) of electricity from three open cast mines. A large percentage of the thermal electricity generated in Tamil Nadu comes from the power plants in Neyveli.



Correspondence to: S. Ghosh  
(satyajitg@vit.ac.in)

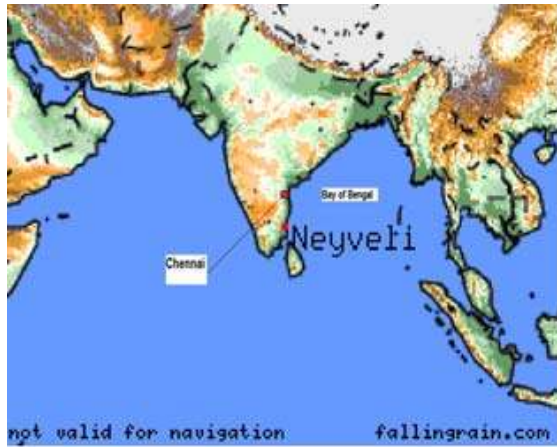


**Fig. 1.** Location of NLC (Latitude – 11°32′-1″ N, Longitude – 79°29′-1″ E).

The origin state Tamil Nadu gets 1,167 MW, while the rest is distributed to other states namely, Andhra Pradesh, Karnataka, Kerala and the union territory of Puducherry (<http://www.nlcindia.co.in>).

The thermal power stations at NLC with corresponding capacities are:

1. Thermal Power Station I (TPS I) = 600 MWPA
2. Thermal Power Station II (TPS II) = 1470 MWPA
3. Thermal Power Station I Expansion (TPS IE) = 420 MWPA

This study applies to Thermal Power Station I only and the stack and emission details given in Table 2 correspond to Stack 1 of TPS I.

### 2.1 Estimating SO<sub>2</sub> concentrations around Stack 1 of TPS I

SO<sub>2</sub> concentrations were generated from a standard Gaussian Plume Model which was coded by us. Emissions of stack 1 of TPS I were treated as an elevated point source (Source strength: 227.8 g/s) with plume rise estimated from formulae adopted by the Bureau of Indian Standards.

The wind measurements were taken at 02:30 p.m. (local time) when the boundary layer was highly unstable. Hence, we chose stability classes A-D (Very Unstable to neutral) for this study conforming to the Pasquill-Gifford stability classes (Seinfeld and Pandis, 2001). This is justifiable; over a hot tropical belt the boundary layer is indeed unstable for much of the time and is generally neutral during precipitation events when the sky is heavily overcast. However, often over NLC, sporadic precipitation events occurred even when the sky was not heavily overcast; appropriate stability classes were chosen to quantify the plume spreads based on the Briggs (1973) formulation.

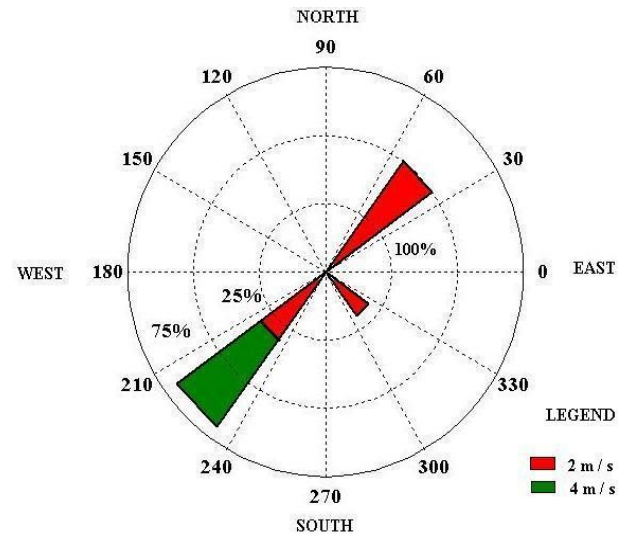


**Fig. 2.** Wind rose for the month of October showing a NE wind component.

**Table 1.** Observed Precipitation intensities at NLC. Rain Rates (R) are in mm hr<sup>-1</sup>.

Month	Total R	Daily (Max.)
Jan-07	0	0
Feb-07	0	0
Mar-07	0	0
Apr-07	50	38
May-07	3.4	3.4
Jun-07	89.4	69
Jul-07	131.8	56
Aug-07	172.2	48
Sep-07	72	31
Oct-07	329.8	122
Nov-07	100	34
Dec-07	298.4	168

### 3 Recreating rain drop spectra from observed rain rates

Three different distribution functions are used to describe rain drop size spectra, namely, the Marshall and Palmer (Marshall and Palmer, 1948), the gamma distribution and the log-normal distribution. A large number of measurements have shown the inadequacy of the M-P model, particularly when the data are averaged over short intervals. Let us first review the commonly used distributions. Marshall and Palmer (1948) characterized rain spectra as an exponentially decaying function:

$$N(D) = N_0 \exp(-\lambda D) \quad (1)$$

**Table 2.** Stack details.

STACK- I PARAMETERS	
Boilers attached	1, 2, 3 each 50 MW
Height in (m)	60
Diameter (m)	2
Flue Gas Velocity (m/s)	20.2
Flue gas exit Temperature (°C)	158
Source Strength (g/s)	227.8

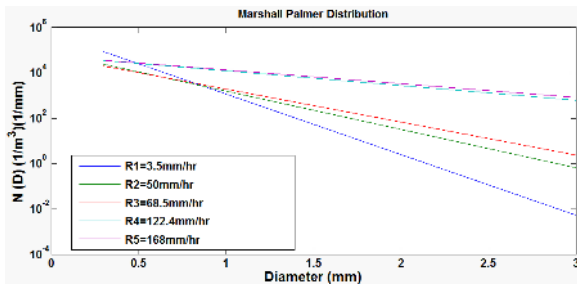


**Fig. 3.** Marshall-Palmer curves for different rainfall intensities over NLC.

Here,  $N_0$  is a constant ( $8000 \text{ m}^{-3} \text{ mm}^{-1}$ ) and  $\lambda$  the slope parameter is a function dependent on the rain rate expressed in  $\text{mm hr}^{-1}$ .  $\lambda$  values for mid latitude precipitation are numerous. They are not as adequately measured for the north eastern monsoonal rains. However, Roy et al. (2005) have reported  $\lambda$  values over a region close to Neyveli. This paper reported  $\lambda$  values for precipitation rates of the order of  $100 \text{ mm/hr}$ . For higher rain rates the  $\lambda$  alues are calculated from Williams and Gage (2009) shown below:

$$\lambda = 4.1R^{-0.21} \tag{2}$$

where R represents rain rate in  $\text{mm hr}^{-1}$ . The rationale behind the use of Eq. 2 is that from observed values of R we estimate  $\lambda$  and feed it to Eq. 1 to get number concentrations. This enables us to plot drop concentration against drop diameters for different rain rates to obtain Fig. 3.

From Fig. 3, we conclude that the highest number of the smallest droplets correspond to low precipitation intensities. It is interesting to note that at the lowest rain rate, the observed slope parameter is such that, some of the smallest drops ( $\sim 0.5 \text{ mm}$ ) are actually more numerous, followed by a steep decline in number concentrations with increasing diameter. For the majority of the droplet sizes spanning diameters between  $0.5\text{--}3 \text{ mm}$ , we observe the intuitive trend i.e. increasing drop number concentrations with increasing precipitation rates. The proportion of larger droplets tends to increase by a factor of two for moderate rain rates (R2 and R3). For the largest rain rates (R4 and R5), frequently encountered during the months of October to December over

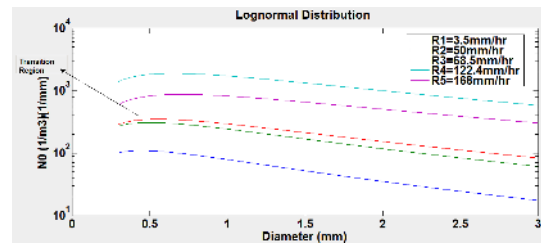


**Fig. 4.** Lognormal curves for different rainfall intensities obtained from NLC data.

Neyveli (although there is a small decrease in the number concentration of the smallest droplets) there is a large increase in the number concentration of the largest droplets up to a factor of six (compare R1 and R5).

The capture of small drops by larger ones results in the fall in drop concentrations. The exponential model as proposed by the Marshall-Palmer distribution is unable to reflect this fall by overestimating the numbers of both very large and very small drops. The main discrepancy arises from the fact that the M-P curves do not show the contributions of the smallest drops accurately-the observed distribution (Roy et al., 2005) clearly shows that the droplet numbers first increase up to a threshold before they begin to fall of exponentially; this feature is not captured by the M-P curves. Discrepancies observed between the Drop Size Distribution (DSD) measurements and the exponential models have led us to use other distributions such as the log-normal distribution which we describe in the next section.

### 3.1 Lognormal distribution

Each DSD data set was fitted with a lognormal distribution function of the form:

$$N(D) = N_T / [(2\pi)^{1/2} (\log \sigma)] \exp[-(\log D / D_m)^2 / 2(\log \sigma)^2] \tag{3}$$

where:  $N_T$ ,  $D$ ,  $D_m$  and  $\sigma$  represents the Total number of droplets, droplet diameter, equivalent diameter and spread of distribution, respectively.

From Eq. 3 we again generate drop concentration as a function of droplet size for specific rain rates. This is shown in Fig. 4.

As expected, we again observe the highest number concentrations for the smallest diameters. Beyond the transition region one observes a steady decline in number concentrations with increasing diameters for all Rain Rates.

Figure 5 shows that the total surface area of small drops overwhelm the surface areas covered by the large drops, because they are more numerous by an order of magnitude, although individual large drops have a larger radii. Thus the small droplets are able to scavenge more SO<sub>2</sub>.

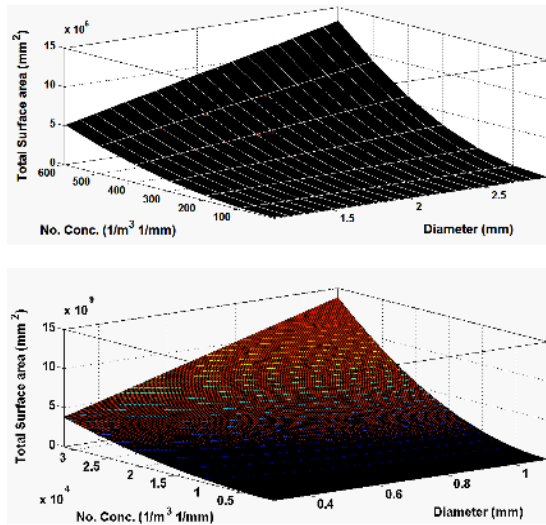


Fig. 5. Total surface area of small and large droplets.

#### 4 Modelling plume washout effects

SO<sub>2</sub> is emitted from a tall elevated stack in a convective boundary layer. During October, winds are moderate as indicated by the wind rose shown in Fig. 2. This facilitates the entrainment and mixing of air. Since we are mainly concerned with the modeling of the washout effects, we multiply the concentration distributions obtained from a Gaussian Plume Model with a term  $e^{-\beta x/u}$  ( $\beta$ ,  $x$ , and  $u$  are the washout coefficient, downwind distance and wind speed respectively). The Gaussian plume model is consistent with the level of sophistication involved in this study. However, we elaborately model the washout term which forms a main component of this study. The term  $e^{-\beta x/u}$  depicts the washout effect, which is essentially time dependent.

In order to retain the simplicity of the Gaussian Plume Model, we parameterized the washout effect as a first order process. However, we noticed that the precipitation intensities are extremely high for monsoonal precipitation and examination of Fig. 4 reveals that there are large as well as small droplets in the droplet spectrum. This fact prompted us to model the washout process comprising polydispersed rain drops rather than monodispersed rain drops. In order to simulate a shower we switch on a precipitation event for a fixed duration of time. In other words, we operate a shower event on a plume of SO<sub>2</sub> travelling downwind at a prescribed speed at the level of the stack.

##### 4.1 Estimation of the washout coefficient

The washout coefficient of a gas in air is the fraction of it removed in unit time by rain below cloud base. The washout coefficient is generally of the order of  $10^{-4} \text{ s}^{-1}$  for mid-latitude precipitation. However, under Indian conditions, the

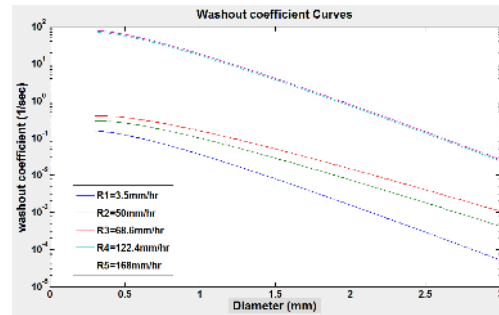


Fig. 6. Variation of washout coefficient with drop size.

washout coefficient could be different and particularly during the monsoon season, when the intensities of precipitation are very high. No work is yet reported in the literature, where the washout coefficients have been calculated for southern India during the NE monsoons. In this paper we have attempted to calculate the washout coefficient for Neyveli.

The washout coefficient is given by (Seinfeld and Pandis, 2001):

$$\beta = (\pi N_T / C_g) \int D^2 N(D) K_y(D) dD \quad (4)$$

where,  $N_T$ ,  $C_g$ ,  $N(D)$ ,  $K_y(D)$  and  $D$  are Total number of rain drops, Gaseous pollutant concentration in air, Drop size distribution by Marshall-Palmer as in Eq. (1), Mass Transfer coefficient and Droplet diameter respectively.

Here  $N_T$ , the total number of rain drops, is calculated from the Marshall Palmer distribution by tabulating the area under the curve for a given rain rate.

##### 4.2 Estimation of the mass transfer coefficient

The mass transfer coefficient is a diffusion rate constant that relates the mass transfer rate, mass transfer area and concentration gradient as the driving force.

The equation to determine mass transfer coefficient (Hales, 1972) is:

$$K_y(D) = 2D_g / D_m [1 + 0.3(D_m U_\infty g / D_g)^{1/2} (\nu / D_g)^{1/3}] \quad (5)$$

where,  $D_g$ ,  $D_m$ ,  $U_\infty$  and  $\nu$  are molecular diffusivity of gas, equivalent diameter of rain droplet, terminal velocity and kinematic viscosity respectively.

The calculated washout coefficients for different precipitation intensities over Neyveli are shown in Fig. 6.

#### 5 Plume washout curves

Figure 7 depicts vertical profiles of the SO<sub>2</sub> concentration for different precipitation events corresponding to showers over NLC. Interestingly, we find that a precipitation intensity of 3.5 mm/hr hardly has any effect on the plume. Higher precipitation intensities cause a depletion of the plume. There

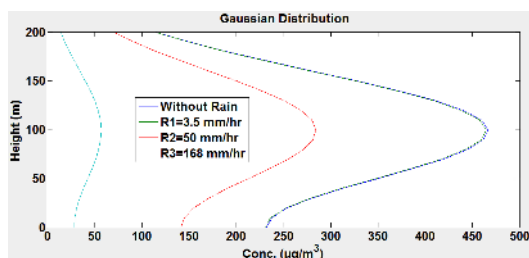


Fig. 7. Vertical Profiles of the depleting Gaussian Plume.

is an 89% depletion of plume when there is a precipitation intensity of 168 mm/hr; this is in sharp contrast to mid latitude precipitation where rain rates are an order of magnitude less. Rain intensities of the kind encountered over Neyveli are fairly typical values for the north east monsoon season: the intense monsoon showers effectively scavenge most of the SO<sub>2</sub> within a few hours. North east monsoonal rain showers typically range from several hours to sometimes even an entire day. Since much of the pollution is partitioned in to the liquid phase it is imperative for us to quantify the amount of dissolved SO<sub>2</sub> brought down by the showers to the ground.

## 6 Wet deposition of SO<sub>2</sub>

In order to proceed to estimate the amount of SO<sub>2</sub> removed due to a precipitant event, we first pick up the most probable raindrop diameter: from Figure 6 this is found to be 1.95 mm. Then we estimate the washout coefficient at a particular rain rate—we show calculations for a rain rate of 168 mm/hr. This is found to be 10<sup>-0.7</sup> per second. The Concentration of SO<sub>2</sub> deposited per unit area of the ground per second ( $C_{\text{removed}}$ ) is obtained as:

$$C_{\text{removed}} = \beta C_T (\mu\text{g m}^{-2} \text{s}^{-1}) \quad (6)$$

Where:  $\beta$  = washout coefficient. ( $\text{s}^{-1}$ ) and  $C_T$  = the total concentration of SO<sub>2</sub> without rain in  $\mu\text{g m}^{-3} \text{s}^{-1}$  obtained by integrating the corresponding vertical Profile of Gaussian curve shown in Figure 7. This yields  $C_T = 928.1 \mu\text{g m}^{-3}$ . Hence,  $C_{\text{removed}} = 185.18 \mu\text{g m}^{-2} \text{s}^{-1}$ .

The above calculations show the cleansing efficiency of the sharp NE monsoon showers—our calculations show that they are comparable to dry deposition rates.

Finally, we would like to comment on how this study fits in with broader concerns. In a commentary, Cracknell and Varotsos (2007) elucidated many aspects of the 4th Assessment Report of IPCC- (2007) (<http://www.ipcc.ch/>). They alluded to the many uncertainties in climate models which included the role of aerosol, clouds and precipitation. In fact, characterizing precipitation accurately is a challenge—this study investigates how NE monsoon showers absorb SO<sub>2</sub> thereby cleansing the atmosphere substantially. Air borne SO<sub>2</sub> is thus brought to the ground. Also, when the smallest

droplets desorb (our study reveals that they are the most numerous), they have the propensity to release SO<sub>2</sub> back to the atmosphere and this could ease the activation of aerosol particles into cloud droplets since SO<sub>2</sub> is a condensable vapour.

Results presented in this paper can be useful for many applications; the most obvious being the corrosive influence of acid precipitation on buildings.

Recent studies by Varotsos et al. (2009) and the references therein testify to the importance of such studies. Varotsos et al. (2009) provide a definitive account of the deleterious effects of acid pollution on the historic buildings in Athens, Greece: they report that weathering of natural stone in Heritage Buildings is exacerbated in the presence of acid deposition. Such studies unfortunately have not been undertaken in Southern India till date; Southern India, in particular the SE part of the coast, boasts of several heritage structures in the form of temples and, like the Acropolis in Greece, a number of ancient monuments. It is expected that when acidic air pollutants are washed down on these stone facades, this will result in corrosion of the façade. The results from this paper amply demonstrate how an accurate quantification of SO<sub>2</sub> washout effects can be achieved when one knows the emission rates and the intensity of precipitation.

## 7 Summary and conclusion

We would like to emphasize that during the north-east monsoon months the wet removal mechanisms are very important. In conclusion we have shown for the first time that for a large lignite based power plant spewing out huge quantities of SO<sub>2</sub> one would expect intolerable levels of air pollution even for a highly turbulent convective boundary layer. This Neyveli case study can be treated as a model study for the Indian sub-continent. The burgeoning population of the sub-continent getting increasingly affluent will continue to consume enormous amount of power. Electricity from fossil fuels will be a major source of production for at least the next five decades – the country's pace of economic growth can not be retarded. The efficacy of the wet removal process is a maximum during north east monsoons. So, wet scrubbers have to be incorporated in the stacks to at least match the sizes and number concentrations of the north east monsoonal rains.

*Acknowledgements.* The authors are grateful to the Office of the Deputy General Manager (DGM), NLC for providing observed data.

Edited by: S. C. Michaelides

Reviewed by: two anonymous referees

## References

- Briggs, G. A.: Diffusion Estimation for Small Emissions, National Oceanic and Atmospheric Administration, ARL Report ATDL-106, 1973.
- Cracknell, A. P. and Varotsos, C. A.: The IPCC fourth assessment report and the fiftieth anniversary of sputnik, *Environ. Sci. Pollut. Res.*, 14(6), 384–387, 2007.
- Ferm, M., Watt, J., O'Hanlon, S., De Santis, F., and Varotsos, C.: Deposition measurement of particulate matter in connection with corrosion studies, *Anal. Bioanal. Chem.*, 384(6), 1320–1330, 2006.
- Hales, J. M.: Fundamentals of the theory of gas scavenging by rain, *Atmos. Environ.*, 6, 635–659, 1972.
- Marshall, J. S. and Palmer, W. M. K.: The distribution of raindrops with size, *J. Meteorol.*, 5, 165–16, 1948.
- Roy, S. S., Datta, R. K., Bhatia, R. C., and Sharma, A. K.: Drop size distribution of tropical rain over south India, *Geol. Geofiz.*, 22, 105–130, 2005.
- Seinfeld, J. H. and Pandis, S. P.: *Atmospheric chemistry and physics*, John Wiley and Sons, 2001.
- Varotsos, C. A., Tzanis, C., and Cracknell, A. P.: The enhanced deterioration of the cultural heritage monuments due to air pollution, *Environ. Sci. Pollut. Res.*, 16, 590–592, 2009.
- Williams, C. R. and Gage, K. S.: Raindrop size distribution variability estimated using ensemble Statistics, *Ann. Geophys.*, 27, 555–567, 2009, <http://www.ann-geophys.net/27/555/2009/>.